

High efficiency active Q-switched laser operation with a large size rectangular core crystalline waveguide

YONGLING HUI,^{1,2,3,4} QI LIU,¹ XING HU,¹ ZHANDA ZHU,^{1,2,3,4} HONG LEI,^{1,2,3,4,5} AND QIANG LI^{1,2,3,4,6}

¹*Institute of Laser Engineering, Faculty of Materials and Manufacturing, Beijing University of Technology, Beijing 100124, China*

²*Key Laboratory of Trans-scale Laser Manufacturing Technology, Ministry of Education, Beijing 100124, China*

³*Beijing Engineering Research Center of Laser Technology, Beijing 100124, China*

⁴*Beijing Higher Institution Engineering Research Center of Advanced Laser Manufacturing, Beijing 100124, China*

⁵*leihong@bjut.edu.cn*

⁶*nctlq@bjut.edu.cn*

Abstract: High efficient pulse output from a large size rectangular core crystalline waveguide actively Q-switched laser was achieved experimentally. A crystalline waveguide, with a rectangular core size of $320\mu\text{m}\times 400\mu\text{m}$ by 1.0at.% Yb:YAG (core), $600\mu\text{m}\times 600\mu\text{m}$ by 0.5at.% Er:YAG (cladding), and $7\text{mm}\times 7\text{mm}$ by 4.0at.% V:YAG (outside of the cladding) was designed and fabricated. Using a continuous diode laser as an end pump, an output pulse energy $1.75\text{mJ}@10\text{kHz}$, pulse width 9.9ns (peak power 175kW), optical-optical efficiency 26%, with the beam quality of $M_x^2=1.15$, $M_y^2=1.10$, were obtained in the experiment. The design method that used to suppress amplified spontaneous emission (ASE) and parasitic oscillation by cutting off the reflection and transmission paths, can be applied for various kinds of crystalline waveguide Q-switched or mode-locked lasers.

© 2021 Optical Society of America under the terms of the [OSA Open Access Publishing Agreement](#)

1. Introduction

High peak power with high brightness for a pulsed and miniaturized laser sources are of particular importance in many applications such as laser materials processing, laser remote-sensing, and long distance free-space optical communication [1–2]. In the process of realizing high peak power output with high brightness, fiber lasers and bulk solid-state lasers encounter different bottlenecks. Fiber lasers have difficulties to obtain high peak power due to tight confinement of the light, that is easy to produce nonlinear effect [3–5]. Bulk solid-state lasers could not achieve high brightness due to adverse thermal effects. Alternative, the crystalline waveguide laser combines the limited output mode as fiber laser and high thermal conductivity of crystal materials, as well as the advantages of high absorption coefficient and high emission cross-section. The crystalline waveguide lasers have potential for high peak power with high brightness output and small volume.

At present, a series of experimental results of CW output crystalline waveguide lasers have been reported [6–8]. The potential of the crystalline waveguide lasers has already been demonstrated for the generation of high optical-optical efficiency and high beam quality with excellent thermal management. Recently, the near diffraction-limited laser CW output from a large size core crystalline waveguide is demonstrated [9], based on the cladding refractive index matching with the core and the core mode competition. In this way, the average output power and the output pulse energy of the crystalline waveguide can be further improved by increasing the

core diameter while maintaining the high beam quality. It is also beneficial to high peak power output of crystalline waveguide laser, when operates in the Q-switched and mode-locked modes. However, there are few reports on high peak power crystalline waveguides laser. Analysis of other types of crystal waveguides, such as the reported single-crystal fiber [10–11], using 1.0at.% Nd:YAG single-crystal fiber, it shows that the optical-optical efficiency are 22% and 9.6% when it operates in the cw and Q-switched regimes respectively [10]. Using 1.0at.% Yb:YAG single-crystal fiber, the continuous output optical-optical efficiency is 38%, while the Q-switched output optical-optical efficiency is 20% [11]. These single-crystal fiber lasers have the same cavity structure, the optical-optical efficiency of the Q-switched output is significantly lower than that of continuous output. This is mainly due to the impact of ASE. In the process of pumping, the randomly emitted photons will be amplified in the gain medium, which consumes the inversion population and reduces the optical-optical efficiency of a Q-switched pulse laser. For the crystalline waveguide, the gain medium in the core layer is surrounded by the cladding and has many reflective surfaces. These surfaces can easily reflect the spontaneous radiation to the gain medium generating parasitic oscillation, especially in the high pump power density condition.

Suppression of parasitic oscillations has been reported for rod and slab geometries using an absorption cladding [12–14]. However, the optical-optical efficiency of quasi-continuous output is only 3.4% higher than that without absorption cladding, and the maximum optical-optical efficiency of passive Q-switching is only 10.2%, which is much lower than the maximum optical-optical efficiency of 62.7% in quasi-continuous operation [14], indicating that the parasitic oscillation is not sufficiently suppressed. It is a motive to design an innovative gain medium geometry for suppressing the ASE and the parasitic oscillation, and realize high energy storage efficiency for high Q-switching optical-optical efficiency crystalline waveguides laser, while keeping good beam quality.

In this paper, a high peak power output is firstly demonstrated from a crystalline waveguide laser with high efficiency. Using a large size core Yb:YAG crystalline rectangular waveguide with a dimension of $320\mu\text{m}\times 400\mu\text{m}$, pulse energy of 1.75mJ, and pulse duration of 9.9 ns are obtained at repetition rates of 10kHz. The maximum output peak power is 175 kW, corresponding to the optical-optical efficiency is 26% with respect to the absorbed pump power of 67W, and the beam quality M^2 value is 1.15×1.10 .

2. Experimental setup

The crystalline waveguide is a single cladding waveguide which is composed of three layers, as shown in Fig. 1. The core layer is 1.0at.% Yb:YAG with a cross-section size of $320\mu\text{m}\times 400\mu\text{m}$, the cladding is 0.5at.% Er:YAG with a cross-section size of $600\mu\text{m}\times 600\mu\text{m}$, and the absorption layer outside of the cladding is 4.0at.% V:YAG with a cross-section size of $7\text{mm}\times 7\text{mm}$. The length of the crystalline waveguide is 76 mm, and the two parallel end faces have an angle of 0.5° relative to the vertical plane of the core layer optical axis.

The 0.5at.% Er:YAG is chosen as the cladding material due to the Er:YAG is fully transparent for the 940nm pump and 1030nm laser, and for the sake of reducing the numerical aperture and increasing the size of the core layer. The refraction index of 0.5at.% Er-doped YAG cladding reduces by only $\sim 4\times 10^{-6}$ with respect to the 1.0at.% Yb-doped core, measured by the interferometry measurement method (the accuracy of $\sim 10^{-7}$) [15]. The small refractive index difference between core and cladding can also increase the critical reflection angle of 1030nm light at the interface between the core and the cladding. The corresponding total reflection angle is 89.88° , i.e. grazing incidence angle is 0.12° . The small grazing incidence angle can reduce the number of times of light reflection at the interface between core and cladding. The cladding cross-section size is designed as $600\mu\text{m}\times 600\mu\text{m}$, for letting the cladding thickness size exceeding the thickness of evanescent wave leakage of the core layer, which is similar to the single clad

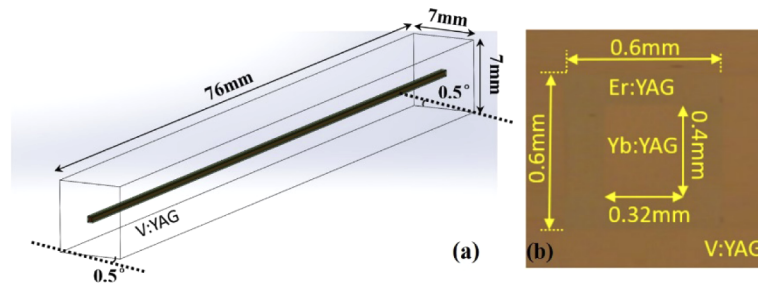


Fig. 1. (a) Structure of the crystal waveguide. (b) The end-face photograph.

waveguide in Ref. [9]. The V:YAG is chosen as the outside of cladding material due to its almost transparency for the 940nm pump laser and absorption for the 1030 nm laser [16]. It is worth noting that this material is used to absorb detrimental ASE light transmitting through the cladding, which is different with that in Ref. [9]. A large dimension 7mm×7mm is selected to effectively absorb ASE and improve the mechanical strength of this waveguide. The 0.5 degree angle of the both end surfaces is used to suppress the parasitic oscillation resulting from the end surfaces residual reflection.

In this novel design, ASE suppression is achieved by cutting off the three types of the parasitic oscillation path. By reducing the refractive index difference between the core layer and the cladding, the ASE light is reflected only once between the interfaces of the core and cladding for small grazing incidence angle, which basically cuts off the path of parasitic oscillation of the interface reflection of the core. By the absorption layer outside the cladding, the ASE light transmitted from each interface of the core layer is cut off. By designing a small angle for the end surfaces, the path of parasitic oscillation due to the end surface residual reflection ASE light is also basically cut off. As a result, ASE suppression can be achieved.

The crystalline waveguide is fabricated by adhesive-free bond (AFB) technology. Both end surfaces of the Yb:YAG crystalline waveguide were anti-reflection (AR) coated for the 940nm and 1030nm wavelength. The crystalline waveguide wrapped in indium foil was clamped between two water-cooled copper blocks for efficient cooling and maintained at 20°C. The pump source is a fiber-coupled diode laser with a center wavelength of 940nm and the maximum power of 135.0W (the core size 105μm, NA 0.22). L1 and L2 are convex lenses with focal lengths of 10mm and 25 mm, respectively, which collimate and focus the pump beam into the waveguide core with the waist spot diameter of 260μm. It should be noted here that the NA of pump light does not match that of the waveguide core, and only part of pump light is absorbed, just as core-pumped. By adjusting the position of pump beam waist in the crystalline waveguide, the absorption rate of the core layer can be as high as possible.

A laser cavity is formed by a 1030 nm high reflection concave mirror M2 and a flat mirror M1 as an output coupler. The optical layout of the Q-switched laser and experimental setup photo are presented in Fig. 2. The plane-concave cavity structure is used to reduce the diffraction loss of the oscillating beam, although the divergence angle of the beam out of the waveguide is small due to the low NA of the waveguide core. The curvature R of concave mirror M2 can

be determined by the transmission matrix, $\begin{bmatrix} 1 & L \\ 0 & 1 \end{bmatrix} \begin{bmatrix} 1 & 0 \\ -2/R & 1 \end{bmatrix} \begin{bmatrix} 1 & L \\ 0 & 1 \end{bmatrix} \begin{bmatrix} R_1 \\ \theta_1 \end{bmatrix}$, where L is the

set distance from the concave mirror surface to the end surface of the waveguide used to place Q-switch elements, and R_1, θ_1 is the beam radius and divergence angle as beams emitted from the end surface of the waveguide. It is assumed that the light emitted from the crystalline waveguide can return to the crystalline waveguide after being reflected by the concave mirror, the curvature

R of the concave mirror M2 can be determined to be 100mm as the setting distance is $L=100$ mm and the beam radius $R_1 = 200\mu\text{m}$.

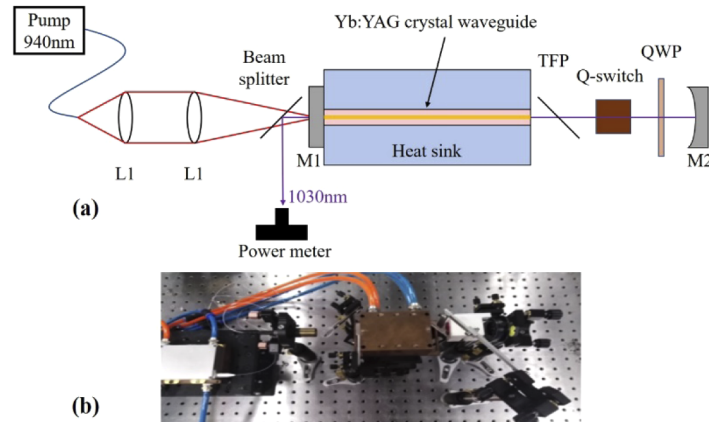


Fig. 2. (a) Experimental setup for pulse output from a crystalline waveguide. (b) The photo of actual setup for pulse output from a crystalline waveguide.

The M1 is anti-reflective to 940nm pump light and 50% reflective to 1030nm light, and close to the left side of the crystalline waveguide end surface. The M2 is placed at a distance of about 100 mm from the right end surface of the crystalline waveguide, with a thin film plate polarizer (TFP), a Pockels cell and a 1/4 wave plate (QWP) between them. A dichroic mirror (beam splitter) is used to separate the output laser and pump light. The size of the Q-switched crystal BBO (Pockels cell) is $\Phi 2.6\text{mm}\times 20\text{mm}$, the 1/4 wave voltage of BBO is 3700V, the rising time of the high voltage electro-optic driver is about 1.0ns, and the Q-switch mode used in the experiment is boosting voltage type. The output pulse characteristics are measured with a power meter, photo-detector and oscilloscope.

3. Experimental results and analysis

Before the actively Q-switched operation, the polarized CW output of the plane-concave cavity is measured, as the Pockels Cell is not driven, and the 1/4 wave plate is adjusted. When the pump power is 135.0W and the pump power absorbed by the waveguide is 67.0W, the polarized laser CW output power of 22.0W is obtained. The results are shown in Fig. 3(a), marked as the new waveguide.

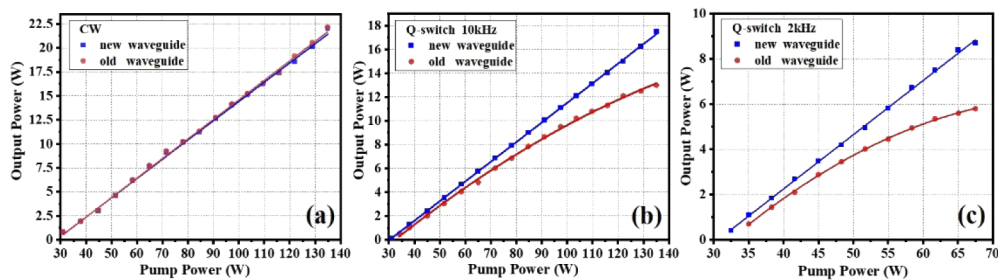


Fig. 3. (a) The CW output power of the polarized laser under different pump power. (b) The output power of the Q-switched laser at 10kHz. (c) The output power of the Q-switched laser at 2kHz.

As the 1/4 wave plate is adjusted and the Pockels cell is driven by the 1/4 wave voltage, the actively Q-switched output is measured. When the pump power absorbed is 67.0W, the average output power is 17.5W and the pulse energy is 1.75mJ@10kHz. The measurement results of Q-switched pulse output power are shown in Fig. 3(b), marked as the new waveguide. The corresponding optical-optical efficiency is 26% and the dynamic to the static ratio of Q-switched operation is 80% (the ratio of output power of Q-switched operation to non-Q-switched operation), which is much higher than that of normal Yb:YAG bulk solid-state actively Q-switched lasers [17–18] and the single-crystal fiber [10–11]. At the maximum pump power, the waveguide output power did not decrease. The results show that the crystalline waveguide laser has the potential of power scalable and high optical-optical efficiency in a Q-switched operation as the pump power is increased.

By adjusting the controller of the Pockels Cell, the Q-switch is operated with smaller repetition rates at 2kHz. The pump power is only half of the maximum power to avoid optical damage. As the pump power is 68.0W and absorbed pump power is 34.2W, the average output power is 8.7W and the pulse energy is 4.35mJ@2kHz. The 2kHz operation results are shown in Fig. 3(c), marked as new waveguide. The optical-optical efficiency is 25.4%, which is almost the same as that of the maximum power with 10kHz repetition rates. For 2kHz operation, the energy storage time of the pump is 5 times longer than that of 10kHz, but the output optical-optical efficiency is not significantly reduced, which indicates that ASE in the crystalline waveguide is effectively suppressed.

In order to further clarify the parasitic oscillation suppression effect of this new waveguide, an old waveguide is used to compare the experiments. The core size and material of the old waveguide is the same as that of the new waveguide, and the core is also surrounded by 0.5at.% Er:YAG cladding, which is described in Yb:YAG waveguide laser in Ref. [9] and [19]. Both waveguides have very similar lengths of 76.0 mm and 77.0 mm. The main difference between the two waveguides is that this new waveguide has a V:YAG absorption layer, while the old one does not. Secondly, the two end surfaces of the new waveguide have an angle of 0.5 degrees, while the old waveguide does not.

Using the old single cladding waveguide replaces the new one for the polarized CW output experiments. As the old waveguide absorbs pump power of 67.0W, the polarized laser CW output power is 22.1W. The results are shown in Fig. 3(a), marked as the old waveguide. The results show that the output of waveguides with or without external absorption layer is similar.

Also using the old single clad waveguide replaces the new one for the actively Q-switching operation experiments, as the waveguide absorbs pump power of 67.0W, the Q-switched average output power is 12.9W and the pulse energy is 1.29mJ@10kHz. The corresponding optical-optical efficiency is 19.3%. The results are also shown in Fig. 3(b), marked as the old waveguide. Comparing the output results, the Q-switched optical-optical efficiency of the new waveguide laser is 6.7% higher than that of the old waveguide laser at the maximum pump power. Changing the Q-switched repetition rate to 2kHz and measuring the output of the old waveguide, as the pump power is 68.0W and absorbed pump power is 34.0W, the average output power is 5.8W and the pulse energy is 2.9mJ@2kHz, the optical-optical efficiency is 17.1%. The measured results are showed in Fig. 3(c), marked as the old waveguide. The Q-switched optical-optical efficiency of the new waveguide is 8.3% higher than that of the old waveguide. The experimental results show that the crystalline waveguide with outside absorption layer is conducive to high-efficiency Q-switched output, it works more effectively when the energy storage density is higher and the storage time is longer.

The pulse width and repetition frequency of the output pulse sequence are measured with a fast photo-detector and an oscilloscope at 10kHz for the new waveguide, as shown in Fig. 4. The measured pulse width is 9.9ns at the maximum output power, corresponding peak power of 175kW@10kHz. The pulse sequence of the actively Q-switched laser has stable amplitude.

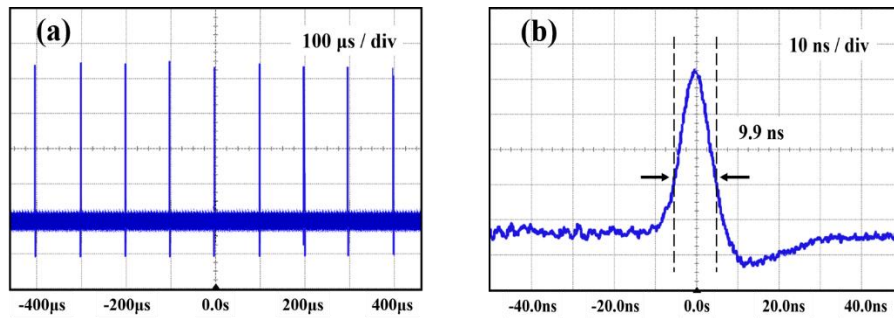


Fig. 4. (a) Actively Q-switched pulse sequence. (b) Actively Q-switched pulse profile.

Although the cross-section of the crystalline waveguide core is rectangular, the far-field spot of the output laser is nearly circular. The output beam quality of the Q-switched pulse at 10kHz was measured by the knife edge method using a CCD camera, which is placed multiple positions after a concave mirror with a radius of curvature of 175 mm and a PBS for attenuation. The beam quality M^2 value in x and y directions are 1.15 and 1.10 at the maximum output power (in Fig. 5). It is verified that large core size rectangular crystalline waveguide Q-switched laser can generate near diffraction-limited beam quality output. The crystalline waveguide core size is larger than that of the fundamental mode core calculated by the traditional method [20]. For 330 μm core layer size where the waveguide includes fundamental transverse mode ($E_{00}^{x,y}$) and higher-order transverse modes such as $E_{01}^{x,y}$, $E_{10}^{x,y}$, $E_{11}^{x,y}$ and $E_{02}^{x,y}$, $E_{20}^{x,y}$, the main composition of the output beam mode is belonging to the fundamental transverse mode. It also can be seen that the core size of the crystalline waveguide in x, y directions are different, but the beam quality in x and y directions are nearly the same. This is due to the increased number of oscillation times in Q-switched laser pulse forming process, and the fierce mode competition.

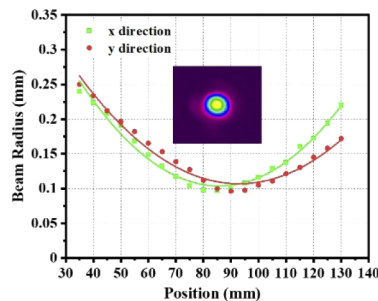


Fig. 5. The beam quality and far-field spot shape of Q-switched laser.

4. Conclusion

In conclusion, we have demonstrated a large size rectangular core crystalline waveguide actively Q-switched laser can generate high peak power pulse, with near diffraction-limited beam quality and high optical-optical efficiency. By designing and fabricating a novel waveguide structure, the reflection and transmission paths of parasitic oscillation are cut off, and the optical-optical efficiency of the crystal waveguide actively Q-switched laser is significantly improved. When the actively Q-switched laser is operated, the output pulse energy is 1.75mJ@10kHz, the pulse width is 9.9 ns, the peak power is 175 kW, and the beam quality M^2 value in x and y directions are

1.15 and 1.10. The optical-optical efficiency of the waveguide laser is 26% with respect to the absorption power of 67.0W. The experimental results show that the large core size rectangular crystal waveguide Q-switched laser has the potential to further improve the peak power with high optical-optical efficiency.

Funding. Natural Science Foundation of Beijing Municipality (4202007, KZ202110005011); National Natural Science Foundation of China (62075003).

Disclosures. The authors declare no conflicts of interest.

References

1. A. Exrance, "Laser weapons get real: long a staple of science fiction, laser weapons are edging closer to the battlefield—thanks to optical fibers," *Nature* **521**(7553), 408–410 (2015).
2. M. N. Zervas and C. A. Codemard, "High power fiber lasers: a review," *IEEE J. Sel. Top. Quantum Electron.* **20**(5), 219–241 (2014).
3. J. W. Dawson, M. J. Messerly, J. E. Heebner, P. H. Pax, A. K. Sridharan, A. L. Bullington, R. J. Beach, C. W. Sidors, C. P. J. Barty, and M. Dubinskii, "Power scaling analysis of fiber lasers and amplifiers based on non-silica materials," *Proc. SPIE* **7686**(1), 768611 (2010).
4. T. A. Parthasarathy, R. S. Hay, G. E. Fair, and F. K. Hopkins, "Predicted performance limits of yttrium aluminum garnet fiber lasers," *Opt. Eng.* **49**(9), 094302 (2010).
5. S. Fu, W. Shi, Y. Feng, L. Zhang, Z. Yang, S. Xu, X. Zhu, R. A. Norwood, and N. Peyghambarian, "Review of recent progress on single-frequency fiber lasers [Invited]," *J. Opt. Soc. Am. B* **34**(3), A49–A62 (2017).
6. N. Ter-Gabrielyan, V. Fromzel, X. Mu, H. Meissner, and M. Dubinskii, "Resonantly pumped single-mode channel waveguide Er:YAG laser with nearly quantum defect limited efficiency," *Opt. Lett.* **38**(14), 2431–2433 (2013).
7. X. Mu, S. Meissner, H. Meissner, and A. W. Yu, "High efficiency Yb:YAG crystalline fiber-waveguide lasers," *Opt. Lett.* **39**(21), 6331–6334 (2014).
8. V. Fromzel, N. Ter-Gabrielyan, and M. Dubinskii, "Cladding-pumped, Yb:YAG-core, fiber-like waveguide laser: modeling and experiment," *Opt. Express* **28**(8), 11899–11910 (2020).
9. X. Hu, D. Cheng, H. Lei, Y. Hui, M. Jiang, and Q. Li, "Near diffraction-limited laser output from a very large size rectangular core crystalline waveguide," *Opt. Lett.* **44**(11), 2685–2688 (2019).
10. J. Didierjean, M. Castaing, F. Balembois, P. Georges, D. Perrodin, J. M. Fourmigué, K. Lebbou, A. Brenier, and O. Tillement, "High-power laser with Nd:YAG single-crystal fiber grown by the micro-pulling-down technique," *Opt. Lett.* **31**(23), 3468–3470 (2006).
11. D. Sangla, I. Martial, N. Aubry, J. Didierjean, D. Perrodin, F. Balembois, K. Lebbou, A. Brenier, P. Georges, and O. Tillement, "High power laser operation with crystal fibers," *Appl. Phys. B* **97**(2), 263–273 (2009).
12. H. Yagi, J. F. Bisson, K. Ueda, and T. Yanagitani, "Y3Al5O12 ceramic absorbers for the suppression of parasitic oscillation in high-power Nd:YAG lasers," *J. Lumin.* **121**(1), 88–94 (2006).
13. A. K. Sridharan, S. Saraf, S. Sinha, and R. L. Byer, "Zigzag slabs for solid-state laser amplifiers: batch fabrication and parasitic oscillation suppression," *Appl. Opt.* **45**(14), 3340–3351 (2006).
14. R. Huß, R. Wilhelm, C. Kolleck, J. Neumann, and D. Kracht, "Suppression of parasitic oscillations in a core-doped ceramic Nd:YAG laser by Sm:YAG cladding," *Opt. Express* **18**(12), 13094–13101 (2010).
15. T. Wu, Y. Hui, Z. Yan, Z. Li, and Q. Li, "Zygo interferometer for the precious measurement of tiny refractive index change of two laser crystals," *Opt. Laser Technol.* **89**, 196–199 (2017).
16. A. M. Malyarevich, I. A. Denisov, K. V. Yumashev, V. P. Mikhailov, R. S. Conroy, and B. D. Sinclair, "V:YAG—a new passive Q-switch for diode-pumped solid state lasers," *Appl. Phys. B: Lasers Opt.* **67**(5), 555–558 (1998).
17. T. Y. Fan, S. Klunk, and G. Henein, "Diode-pumped Q-switched Yb:YAG laser," *Opt. Lett.* **18**(6), 423–425 (1993).
18. J. Liu, J. Xin, Y. Lang, and J. Chen, "Multiple folded resonator for LD pulse end pumped Q-switched Yb:YAG slab laser," *Opt. Express* **22**(18), 22157–22162 (2014).
19. D. Cheng, X. Hu, H. Lei, Y. Hui, M. Jiang, and Q. Li, "Design and experimental verification of near diffraction-limited output of a large core size Yb:YAG crystalline waveguide laser," *Opt. Commun.* **451**, 307–310 (2019).
20. J. I. Mackenzie, C. Li, D. P. Shepherd, H. E. Meissner, and S. C. Mitchell, "Longitudinally diode-pumped Nd:YAG double-clad planar waveguide laser," *Opt. Lett.* **26**(10), 698–700 (2001).